

Computationally-Effective Worst-Case Model of Wire Radiation in the Frequency Range 1 Hz - 40 GHz

Arlou Y.Y.¹, Sinkevich E.V.¹, Maly S.V.², Slepyan G.Ya.³

¹ EMC R&D Laboratory, Belarusian State University of Informatics and Radioelectronics, Minsk, Belarus, emc@bsuir.by

² The Faculty of Radiophysics and Computer technologies, Belarusian State University, Minsk, Belarus, maly@bsu.by

³ School of Electrical Engineering, Tel-Aviv University, Tel-Aviv, Israel, gregory_slepyan@yahoo.com

Abstract—The worst-case model of a wire radiation field intended for the analysis of spurious couplings in complexes of radio and electronic equipment has been developed. The model is based on dividing the wire into straight-line segments and considering forward and backward current waves in each segment. The solution for each current wave is interpreted as interference of fields radiated by equivalent point sources, and the envelope of the amplitude-frequency characteristic is found in the area of resonances. The correctness of the model is checked in a wide range of problem parameters values: the length of the wire ranges from 0.1 m to 10 m, the height of the wire above the ground plane ranges from 0.1 mm to 1 m, and the observation point position is up to 10 m away from the center of the wire in arbitrary direction.

Index Terms—wire radiation; frequency response; worst-case model; envelope

I. INTRODUCTION

Radiation of connecting wires may cause a significant electromagnetic interference [1]. The wire radiation models known to the authors have the following limitations making these models inapplicable for express analysis of EMC [2], [3]. The field calculation by the methods of computational electromagnetics is too slow. Moreover, the computed field distribution is jagged by interference effects at high frequencies. The field irregularity makes the model unstable since small errors in model parameters values may cause significant changes of the computed field. Analytical electrodynamic models (e.g., given in [4], [5]) provide an opportunity of a fast calculation of the wire field (both at low and high frequencies), but the calculated field is also jagged. The statistical approach (e.g., Monte-Carlo method) can be used for removing the computed field irregularity at high frequencies, but it requires a lot of iterations, so it is computationally ineffective even if an analytical electrodynamic model is applied at each iteration [6]. Worst-case models based on Hertzian dipole can be used only for electrically short wires [1]. A number of analytical models make it possible to obtain the worst-case estimation of the field in the far-field zone but they are inapplicable in the near-field zone [1].

The objective of this paper is to design a computationally-effective worst-case model of radiation from the wire located

within metallic chassis of an on-board system (aircraft, ship, van, etc). The model is intended for express analysis of EMC in the frequency range of 1 Hz – 40 GHz, so it must be applicable in the near-field and far-field zones for wires of any wave dimension. While choosing the model frequency range, we follow [7] (RE101 limit: Radiated Emissions, Magnetic Field, 30 Hz to 100 kHz; RE102 limit: Radiated Emissions, Electric Field, 10 kHz to 18 GHz) and the frequency range of system-level EMC modeling in “EMC-Analyzer” software [3].

For express analysis of EMC in the frequency domain, it is necessary to calculate the field amplitude in a specified observation point at a given set of frequencies [2], [3], i.e., the amplitude-frequency characteristic (AFC) of the field. Therefore, it is also required to design a computationally-effective algorithm for calculation of the field AFC according to the developed model.

The paper is organized as follows. The statement of the problem and the approximations being used are described in Section II. Section III contains an exact solution to the problem from Section II. Development of the worst-case model based on the exact solution is described in Section IV. The model validation results are given in Section V.

II. PHYSICAL MODEL

A high speed of computation that is required for the model can be achieved only by taking into account the most important factors of a real-world problem. Thus, we developed a physical model accounting for such factors (Fig. 1).

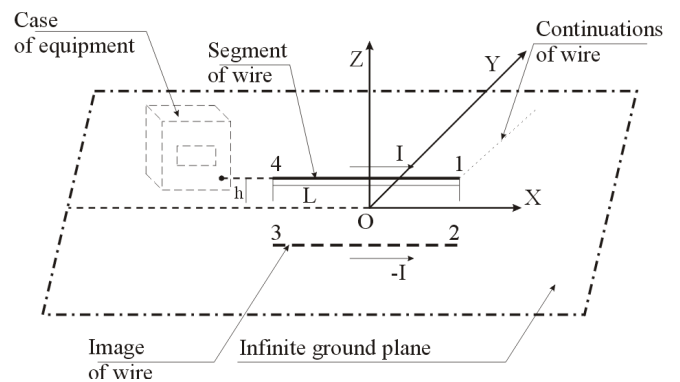


Figure 1. Physical model of the problem

On-board systems, for which the given model is intended, have a metallic chassis. The chassis reflects electromagnetic fields and has a significant effect on the resulting field. Therefore, we take into account the chassis of an on-board system. The wires influence of which on EMC of on-board equipment need to be estimated connect the equipment together. Such wires are usually laid near to the floor and walls. Therefore, we suppose that the nearest surface of the system chassis has the maximal influence on the field, and the chassis is modeled by an ideal infinite ground plane. This makes it possible to take the chassis into account by means of the method of images [8] (i.e., to consider the image of wire instead of the ground plane. This image is placed symmetrically with respect to the ground plane and has current distribution displaced in phase by π relative to current distribution in the wire).

The wire is considered as a set of straight-line segments. Each segment is analyzed separately, and the sum of absolute values of the segments fields is taken (otherwise the total field can be jagged, and the model becomes unstable. See Introduction).

It is supposed that the wire is placed in parallel to the ground plane at a height h (the averaged height is used [2]). Radius of the wire is assumed to be many times less than h , the length λ of an electromagnetic wave, a segment length L , and the distance from the wire to the observation point. Velocity v_s of the signal propagation along the wire is assumed equal to light velocity c in free space (wire covering is not taken into account in this work).

Current which propagates along the wire also permeates through the equipment to which the wire ends are connected. The developed model describes radiation from (open) current passing through the wire only, because the field radiated by the equipment is taken into account by other models when the express analysis of EMC is performed [2], [3].

In order to obtain analytical formulas for the field, it is necessary to approximate real current distribution along the wire by some simple model. In this paper, current distribution is approximated by a sum of two current waves propagating along the wire in the opposite directions:

$$I_x(x) = C_1 e^{jkx} + C_2 e^{-jkx}, \quad j = \sqrt{-1}, \quad k = 2\pi/\lambda, \quad (1)$$

where C_1 and C_2 are the amplitudes of the current waves (they are input data for the developed model, e.g., they may be computed by means of the transmission line theory), k is the wave number.

According to the worst-case principle, fields of the current waves are summed without taking into account their phases.

Below, the calculation of the field radiated by the current wave propagating in the direction of coordinate x increasing (i.e., $C_1 = 0$ - see Fig. 1) is investigated.

III. EXACT SOLUTION

A. Full model

If $C_1 = 0$ and $C_2 = I_0$ then current distribution (1) along the wire has the following form:

$$I_x(x) = I_0 e^{-jkx}. \quad (2)$$

After computing electromagnetic field of current wave (2) by means of vector potential [9], one obtains

$$F_a = I_0 e^{jkx_0} \sum_{i=1}^4 F_{ai}, \quad (3)$$

where F_a is the projection of the field F ($F \in \{E, H\}$) onto the coordinate axis a ($a \in \{x, y, z\}$), namely

$$\begin{pmatrix} E_{xi} \\ E_{yi} \\ E_{zi} \end{pmatrix} = (-1)^{i+1} \frac{e^{-jk(r_i - r_{xi})}}{4\pi\epsilon_0\omega r_i} \begin{pmatrix} r_{xi} \{jk(1/r_i + 1/r_{xi}) + 1/r_i^2\} \\ r_{yi} \cdot \xi \\ r_{zi} \cdot \xi \end{pmatrix}, \quad (4)$$

$$\xi = jk \{1/r_i - 1/(r_i - r_{xi})\} + 1/r_i^2;$$

$$\begin{pmatrix} H_{xi} \\ H_{yi} \\ H_{zi} \end{pmatrix} = (-1)^{i+1} \frac{e^{-jk(r_i - r_{xi})}}{4\pi r_i(r_i - r_{xi})} \begin{pmatrix} 0 \\ -r_{zi} \\ r_{yi} \end{pmatrix}, \quad (5)$$

where r_i is the distance between the i -th wire (or its image) end and the observation point (x_0, y_0, z_0) ; r_{xi} , r_{yi} and r_{zi} are x , y and z projections of this distance, respectively: $r_i = |\vec{r}_i|$, $\vec{r}_i \equiv (r_{xi}, r_{yi}, r_{zi})$.

According to given formulas, the field of the physical model consists of four summands when one current wave is considered. Every summand is dependent on the radius-vector \vec{r}_i which connects the i -th wire (or its image) end and the observation point, and it is independent of other spatial variables. Therefore, the field radiated by the wire can be interpreted as a sum of fields of fictitious point sources placed at the wire and its image ends. This interpretation has the following advantage: one long wire is replaced by two point sources the field amplitude and phase of which are described by simple formulas. The analysis of interference effects for a small number of point sources is much simpler than the analysis for a long object.

B. Electric field spikes at the wire ends. Truncated model

Current distribution in the physical model has discontinuity at the wire ends (see Section II), which means the presence of electric charges at the wire and its image ends. The amplitude

of the charge q_i is equal to I_0/ω . As a result, the field of the charges is

$$Ech_a = I_0 e^{jkx_0} \sum_{i=1}^4 Ech_{ai}, \quad (6)$$

where

$$\begin{pmatrix} Ech_{xi} \\ Ech_{yi} \\ Ech_{zi} \end{pmatrix} = (-1)^{i+1} \frac{e^{-jk(r_i - r_{xi})}}{4\pi\epsilon_0\omega \cdot r_i^3} \begin{pmatrix} r_{xi} \\ r_{yi} \\ r_{zi} \end{pmatrix}. \quad (7)$$

At $\omega \rightarrow 0$ the electric field (7) tends to infinity. Therefore, at low frequencies the field will have spikes near the wire and its image ends (points of electric charges accumulation). But in the real situation these charges flow from the wire segment because the segment is connected to other conductors. Therefore, it is necessary to exclude field (7) of charges from consideration. Formulas (4) without the field of charges are the following

$$\begin{pmatrix} E_{xi} \\ E_{yi} \\ E_{zi} \end{pmatrix} = (-1)^{i+1} \frac{e^{j\pi/2 - jk(r_i - r_{xi})}}{4\pi\epsilon_0 c \cdot r_i^2} \begin{pmatrix} r_{xi} + r_i \\ -r_{xi}r_{yi}/(r_i - r_{xi}) \\ -r_{xi}r_{zi}/(r_i - r_{xi}) \end{pmatrix}. \quad (8)$$

Amplitudes of the fictitious sources in (8) are independent of frequency, and frequency dependency of the field is determined only by phase relationships between the fictitious sources.

C. Numerical errors

According to (5) and (8), the field amplitudes of certain sources tend to infinity near to the wire axis (i.e., if $|r_i - r_{xi}| \rightarrow 0$). But if the observation point is not located inside the wire ($|r_{xi}| > L/2$), then the total field must tend to a certain finite value (because the field cannot be infinite if the observation point is located in free space and is not adjacent to some other objects). Therefore, special formulas are necessary for the field calculation at points located close to the wire axis. We can derive these formulas by expanding the total field created by four fictitious sources as a power series of distance between the observation point and the wire axis and retaining the first terms of the series. The volume of the paper did not allow us to give the derived expression.

IV. WORST-CASE MODEL

A. Modeling the AFC envelope

a) Principle of the calculation

Since expressions (8) without the phase multiplier $\exp(j\pi/2 - jk(r_i - r_{xi}))$ are independent of frequency, we see that the envelope for the AFC of two fictitious sources can be found by using the sum of absolute values of the sources field

amplitudes. But if the summed fields are antiphased at low nonresonance frequencies, then the described procedure will lead to overestimation of the field level at these frequencies. Therefore, it seems reasonable to compute the envelope only at frequencies higher than the frequency of the AFC first maximum. The sum of absolute values of the fields radiated by two fictitious sources is equal to their vector sum at the frequency of the AFC maximum (because the fields are cophasal). This implies continuity of the resulting AFC.

b) Zones of AFC

Hereinbefore we divided the AFC into two frequency domains (below or above the first maximum of the AFC). This made it possible to introduce a binary criterion «jagged – not jagged» for two sources. If there are four sources, then six different pairs of sources can be selected, i.e., a six-bit criterion of AFC irregularity can be introduced. It is convenient to represent such a criterion by a graph in which vertexes correspond to fictitious sources and the absence of the edge between two vertexes indicates that the corresponding bit in the criterion has value «jagged».

Let us define a zone of the AFC as a frequency interval in which the given class of isomorphism for the graph is unchanged (Fig. 2). Each zone needs its own way for enveloping the AFC.

c) Analytical envelope

Analytical formulas of envelopes are found for 5 zones out of 11 possible zones by the use of the following principle: if two sources are represented by adjacent vertexes of the graph, then their fields must be summed vectorially, otherwise the sum without taking into account summands phases must be used. For example, if the field only of sources 1 and 2 is not jagged, then the formula for the total field envelope is:

$$F^{5A}_a = |F_{a1} + E_{a2}| + |F_{a3}| + |F_{a4}|. \quad (9)$$

The other formulas for the analytical envelope of AFC are as follows (numeration of the sources is relative):

$$\begin{aligned} F^{0A}_a &= |F_{a1} + F_{a2} + F_{a3} + F_{a4}| \\ F^{3A}_a &= |F_{a1} + F_{a2} + F_{a3}| + |F_{a4}| \\ F^{4B}_a &= |F_{a1} + F_{a3}| + |F_{a2} + F_{a4}| \\ F^{6A}_a &= |F_{a1}| + |F_{a2}| + |F_{a3}| + |F_{a4}| \end{aligned} \quad (10)$$

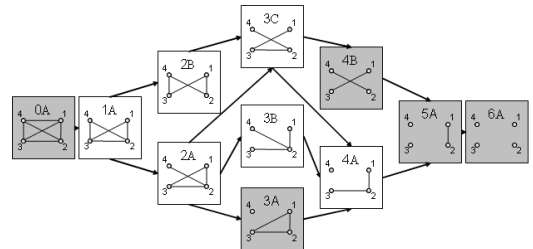


Figure 2. Types of graphs for the AFC irregularity criterion for all possible zones of the AFC, and transitions between them with increasing the frequency

d) Numerical algorithm for envelope calculation

For the other 6 zones a numerical algorithm of enveloping is developed, which allows one to calculate a nondecreasing AFC between two analytically enveloped zones with gradual frequency transition between their analytical formulas of envelopes. This algorithm uses linearly spaced nodes in the logarithmic frequency scale and linear interpolation between the values of nodes in this scale.

e) Algorithm of the AFC calculation for a set of frequencies

An optimized algorithm is developed for fast calculation of the whole AFC. It is based on precomputation of the following: 1) amplitudes of the fictitious sources; 2) sequence and frequency boundaries of the AFC zones; 3) correspondence between the numbers of the fictitious sources and the numbers of the terms in expressions (10); 4) values of nodes for the numerical algorithm from the paragraph d). Testing showed the twenty times (average) increase in the AFC calculation speed due to the precomputation.

B. Elimination of notches in the spatial distribution of the field at low frequencies

The electric field (8) spatial distribution has narrow notches at low frequencies (Fig. 3).

The investigation of the field dependency on the signal propagation velocity v_s along the wire has shown that at low frequencies the amplitude of the electric field depends on v_s under the law $E(v_s) \equiv |A + B \cdot v_s|$, where A and B are quantities independent of v_s . There are points at which the field is close to zero at $v_s = c$. If we remove the constant A from the dependency $E(v_s)$, then the field will be proportional to v_s and will not be equal to zero when $v_s = c$. The formulas for the electric field having this property are as follows:

$$\begin{pmatrix} E_{mod_{xi}} \\ E_{mod_{yi}} \\ E_{mod_{zi}} \end{pmatrix} = (-1)^{i+1} \frac{e^{j\pi/2 - jk(r_i - r_{xi})}}{4\pi\epsilon_0 cr_i} \begin{pmatrix} 1 \\ -r_{yi}/(r_i - r_{xi}) \\ -r_{zi}/(r_i - r_{xi}) \end{pmatrix}. \quad (11)$$

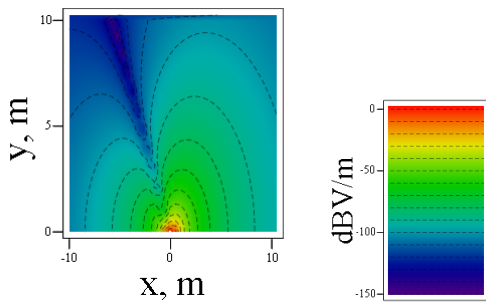


Figure 3. Distribution of the electric field in z-plane, as computed by the truncated model (8). Model parameters: $z=1$ mm, $L=1$ m, $h=0.1$ m, $f=10$ Hz, $I=1$ mA

Expressions (11) make it possible to avoid the notch described above. But the total field calculated by (11) is less than the field calculated by initial expressions (8) in certain spatial ranges. So, the worst-case value of the field is taken as a maximum of the two values calculated by (8) and by (11).

C. Estimation of computational efficiency

First we compared the computational efficiency of the worst-case model and of exact analytical model (8). This is done by computation of the AFC consisting of 10^5 points for the electric field. In order to estimate the uncertainty of the computing time measurement, the computation of the AFC is performed 5 times for each model. For the worst-case model, the average computing time per one point of the AFC is 32.7 μ s and the range of sample is 12.9 μ s. For the exact analytical model, they are 33.4 μ s and 5.6 μ s, correspondingly. So, the times of the AFC computation by the worst-case model and by the exact model can be considered as equal within errors.

Then we compared the calculation speed of the worst-case model and of a computational electromagnetics model (implemented by the method of wire discretization into Hertzian dipoles [9]). The comparison is carried out for the AFC consisting of 1000 points. The number of Hertzian dipoles for the wire discretization is calculated as $5000 + 500L/\lambda$ (because the large number of discretization elements is needed for computation of the field near to the wire). The average computing time per one point of the AFC is 91 ms for the computational electromagnetics model, and it is 3 orders of magnitude less (63 μ s) for the worst-case model.

Monte-Carlo method together with a statistical model of the problem parameters variability can be used for removing irregularity of the field computed by the exact (analytical or numerical) model (see Introduction). In this case, multiple calculations (about 20...60 iterations [6]) of the AFC and subsequent selection of the maximal field value in each point of the AFC among all realizations are required in order to compute the envelope. Therefore, the computation speed for the worst-case model proposed here is roughly 1-2 orders of magnitude higher than for the Monte-Carlo model involving the exact analytical model. And the computation speed for the worst-case model is 4-5 orders of magnitude higher than for the Monte-Carlo model involving the numerical model.

All models used for the comparison of computational efficiency are implemented in c++. Executable files corresponding to the models are built with the same compiler settings. The test computer has the following characteristics: the processor is AMD FX(tm)-4100 Quad-Core (one core is used for the computations), the RAM size is 3 GB.

V. MODEL VALIDATION

A. Validation of the truncated model

1) Initial validation

The absence of mathematical errors and correctness of programming for the truncated model were validated by comparing the results of calculation by (5) and (8) with the results of simulation by wire discretization into Hertzian dipoles. The current in the wire was set in accordance with (2),

and current in the image was shifted in phase by π relative to (2).

2) Validation by means of general-purpose methods of computational electromagnetics

According to Section II, the developed model calculates the open current field. But if one wants to calculate a field by a general-purpose method of computational electromagnetics, then he must extend the physical model (given in Section II) in such a way that the current is closed. The simplest suitable extension of the physical model is adding two vertical wires connecting the ground plane and the ends of the existing wire; the current source is placed at one of the vertical wires, and the load is placed at the second vertical wire. If one wants to form only one current wave (see Section II) then the resulting transmission line must be matched. The matching is achieved by adjusting of the load resistance.

In order to calculate the field of the extended physical model by the truncated model (5) and (8), we must add the field calculated by the truncated model to the field radiated by the vertical wires. Expressions for the field of one wire can be derived from the truncated model (5) and (8) by taking the fields radiated by the 1st and 4th sources (ref. Fig. 1). Then the field of the vertical wire placed in the required spatial position can be determined by applying transformations of coordinates to the expressions obtained.

The examples of spatial distributions for the electric and magnetic fields calculated on the base of the extended physical model by the method of moments [10] and by the truncated model (5) and (8) are shown in Figs. 4 and 5. The examples of AFCs for the electric and magnetic fields calculated by the truncated model and by the method of moments are shown in Figs. 6 and 7, respectively: here we cannot observe resonances at high frequencies of the given AFCs (because of insufficiently dense grid for values of their argument), but we can check correctness of the AFC computation at the grid points. Figure 7 demonstrates satisfactory fit of the results for the electric and magnetic fields.

Thus, applicability of formulas (5) and (8) to calculation of the field radiated by the wire segment is shown.

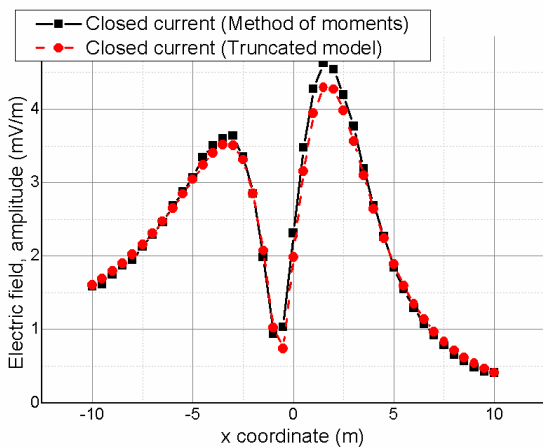


Figure 4. Distribution of the electric field along x coordinate. Model parameters: $L=1.3$ m, $h=0.04$ m, $y=3$ m, $z=3$ m, $f=200$ MHz, $I=1$ mA

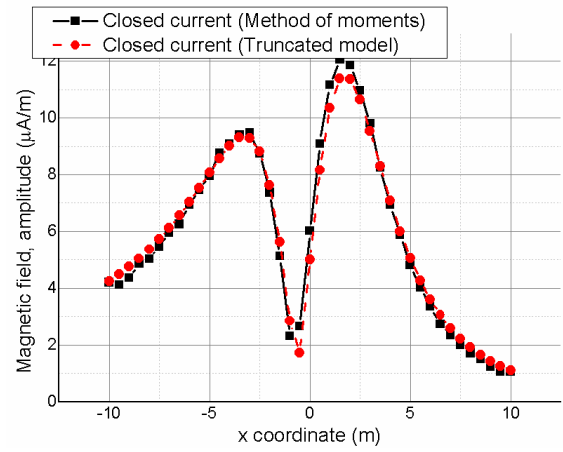


Figure 5. Distribution of the magnetic field along x coordinate. Model parameters: $L=1.3$ m, $h=0.04$ m, $y=3$ m, $z=3$ m, $f=200$ MHz, $I=1$ mA

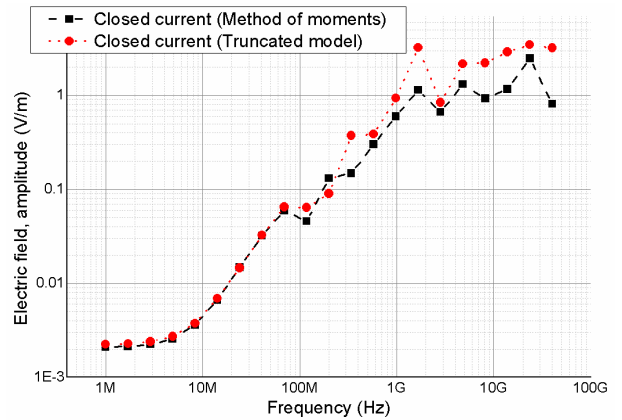


Figure 6. The AFC of the electric field. Model parameters: $L=1.3$ m, $h=0.04$ m, $x=-3$ m, $y=0.02$ m, $z=3$ m, $I=1$ mA

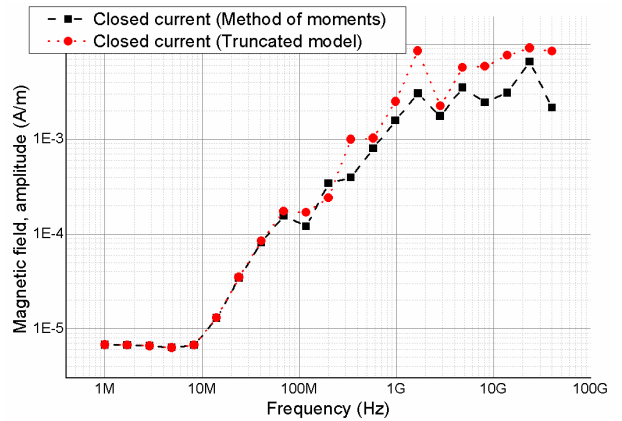


Figure 7. The AFC of the magnetic field. Model parameters: $L=1.3$ m, $h=0.04$ m, $x=-3$ m, $y=0.02$ m, $z=3$ m, $I=1$ mA

B. Validation of the worst-case model

Since the physical model field (see Section II) cannot be evaluated directly by means of general-purpose methods of computational electromagnetics, we decided to validate the worst-case model by comparison with the truncated model (the correctness of the truncated model is shown in Section V.A).

The worst-case model was implemented in c++ and it was verified by a visual check of the AFC envelope quality for more than 400 test cases (besides, the envelope for spatial distribution of the field was verified). The choice of test cases was based on the following restrictions: the frequency ranged from 1 Hz to 40 GHz, the wire length ranged from 10 cm to 10 m, the wire height above the ground plane ranged from 0.1 mm to 5 m, and the size of the field calculation space was up to 10 m. The following 5 values of the h/L ratio (from minimal to maximal) were chosen: 10^{-5} , $5 \cdot 10^{-3}$, $5 \cdot 10^{-2}$, $5 \cdot 10^{-1}$, 50. The points in which the test calculation of the AFC was performed are shown in Fig. 8.

The examples of the AFCs calculated by the truncated and worst-case models are shown in Figs. 9 and 10 (the model parameters correspond to the parameters used in Figs. 6 and 7). For the other test cases, we have not found optimism or excessive pessimism either. The AFC envelope calculated by the worst-case model is not jagged in all cases.

VI. CONCLUSION

The worst-case model of the wire radiation field in the frequency range 1 Hz – 40 GHz applicable in the near-field and far-field zones is developed. The model can be applied for express analysis of the EMC between on-board radio and electronic equipment of a car, aircraft, ship, etc. [2], [3].

We have shown that the model is correct, worst-case, and computationally effective.

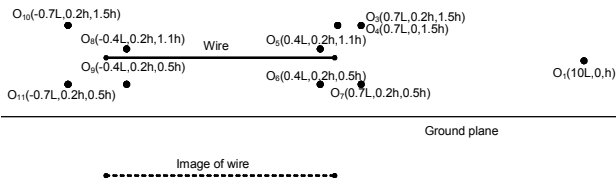


Figure 8. Positions and coordinates of points in which the worst-case model of the AFC of the field radiated by the wire was tested

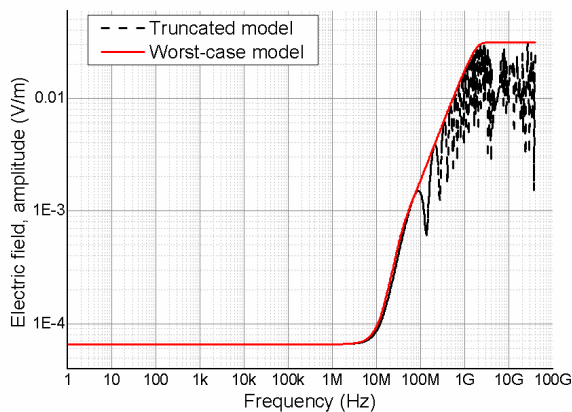


Figure 9. The AFC of the electric field radiated by the wire segment. Model parameters: $L=1.3$ m, $h=0.04$ m, $x=-3$ m, $y=0.02$ m, $z=3$ m, $I=1$ mA

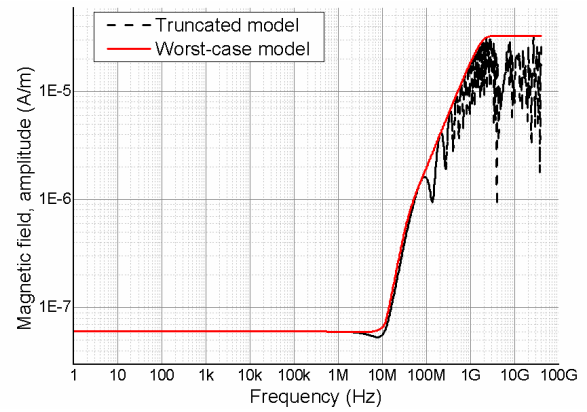


Figure 10. The AFC of the magnetic field radiated by the wire segment. Model parameters: $L=1.3$ m, $h=0.04$ m, $x=-3$ m, $y=0.02$ m, $z=3$ m, $I=1$ mA

REFERENCES

- [1] C. R. Paul, "Introduction to Electromagnetic Compatibility," 2nd ed., Wiley, Hoboken, NJ, 2006, 983 p.
- [2] J. L. Bogdanor, R. A. Pearlman, M. D. Siegel, "Intrasystem Electromagnetic Compatibility Analysis Program: Volume I," User's Manual Engineering Section, McDonnell Douglas Aircraft Corp., F30602-72-C-0277, Rome Air Development Center, Griffiss AFB NY, Dec. 1974.
- [3] EMC-Analyzer. Mathematical models and algorithms of electromagnetic compatibility analysis and prediction software complex. Minsk, 2013.
- [4] M. Chaaban, K. El K. Drissi, D. Poljak, "Analytical model for electromagnetic radiation by bare-wire structures," Progress In Electromagnetics Research B, 2012, Vol. 45, pp. 395-413.
- [5] B. C. Tseng, L. C. Liao, L. K. Wu, H. T. Lung, "Analytical Solutions for the Radiated Emission of Parallel Microstrip Traces," IEEE Trans. on EMC, vol.53, No.3, pp. 842-845, August 2011.
- [6] E. Yavolovskaya, S. Iosava, T. Injgia, Z. Sukhiashvili, and R. Jobava, "Methodology for consideration of stochasticity effects in cable bundles on radiated emission problems," Direct and Inverse Problems of Electromagnetic and Acoustic Wave Theory, 2009. DIPED 2009. International Seminar/Workshop on, pp. 44-48. IEEE, 2009.
- [7] MIL-STD-461F, "USA Department of Defense Interface Standard, Requirements for the Control of Electromagnetic Interference Characteristics of Subsystems and Equipment", 10 December 2007
- [8] R. J. Low, "Electrodynamics, differential forms and the method of images," Eur. J. Phys, 32, 2011, pp. 1413-1417.
- [9] J. D. Jackson, "Classical electrodynamics," New York: Wiley, 1962, 641 p.
- [10] R. F. Harrington, "Field computation by moment methods," New York: IEEE Press, 1993, 211 p.